Nonlinear RF Pulse Optimization for Segmented Multi-Dimensionally Selective Excitation with Parallel Transmit

Martin Haas[1], Jeff Snyder[1], Jürgen Hennig[1], and Maxim Zaitsev[1]
[1]*Department of Radiology, Medical Physics, University Medical Center Freiburg, Freiburg, Germany*

Introduction

For multi-dimensional selective excitation, the duration of the encoding trajectory in transmit k-space is an important limiting factor. Off-resonance artifacts and the decay of magnetization during transmit significantly impair the selection quality. Although correction methods exist for these problems [1, 2] they can handle limited disturbances only and usually increase the RF power. In addition, for localization in MR spectroscopy, the correction of these effects at the water frequency is not enough to achieve the desired excitation pattern for a broad frequency range. Parallel transmit [3-5] can be used to reduce the pulse duration as such, but usually not enough for good broadband excitation. To significantly increase the bandwidth of the selection, a division of RF pulses into segments across several repetitions has been demonstrated [6] and generalized to large tip angles on a segment-by-segment basis [7]. In this work, we extend these methods by optimizing the segmented RF pulse as a whole and thus arrive at a general nonlinear RF pulse design on segmented trajectories.

Methods

The small tip angle (STA) approximation in RF design implies that magnetization contributions generated at different points of time along the transmit k-space trajectory add up linearly. Therefore, an STA pulse can be split up into multiple segments and the resulting magnetization patterns $M_s(T, \mathbf{r})$ added without modifications, as long as the k-space trajectory of each segment starts (and ends) at the k-space origin ($s = 1..N$, $N =$ number of segments, $T =$ duration of segments). To arrive at a 90° excitation tip angle, single segment pulses can be further optimized using an optimal control solution of the full Bloch equation [8] to scale up not the flip angle but the magnetization patterns, keeping the relative magnitudes of the M_s fixed [7]. Upon addition of the $M_s(T, \mathbf{r})$, the desired target pattern is then obtained with large transverse magnetization. However, this method uses a partition of the target pattern into sub-patterns M_s based on the STA approximation. To lift this restriction, in the present work STA pulses are still used as an initial guess, but the optimal control algorithm as presented in [8] is adapted to minimize a cost function that includes all segments simultaneously. To that end, the Lagrangian multipliers $\boldsymbol{\lambda}$ and the error norm ϕ are expressed in terms of the difference of the transverse magnetization $\mathbf{M}_t$ summed over the segments and the target vectors $\mathbf{D}$:

$$\boldsymbol{\lambda}(T, \mathbf{r}) = \mathbf{M}_t(T, \mathbf{r}) - \mathbf{D}(\mathbf{r}) = \sum_{s=1}^{N} \begin{pmatrix} M_{s,x}(T, \mathbf{r}) \\ M_{s,y}(T, \mathbf{r}) \\ 0 \end{pmatrix} - \begin{pmatrix} D_x(\mathbf{r}) \\ D_y(\mathbf{r}) \\ 0 \end{pmatrix},$$

where in each iteration, $M_{s,x}$ and $M_{s,y}$ result from a forward integration of the Bloch equations for each segment. No condition is imposed on the z-component of the magnetization. Thus the M_s are allowed to vary as a function of location $\mathbf{r}$ during the optimization and thus contribute to a further reduction of the error norm ϕ.

Results and Discussion

Figure 2 shows some of the magnetization patterns M_s as resulting from the segment-wise optimization and from the generalized algorithm. The differences are small but non-negligible, demonstrating that the degrees of freedom in partitioning the target pattern are indeed used in the generalized optimization. Figures 3 and 4 show the simulated transverse magnetization after all segments are played out and the signals added. The generalized algorithm shows improved excitation fidelity as compared to the STA and the segment-wise optimized RF pulse design. This technique is especially useful in MR spectroscopy where many averages need to be made, and the multiple TRs can be used for cycling through the segments.

Conclusion

We have shown how segmented multi-dimensionally selective excitation pulses can be obtained with large tip angle using the additional degrees of freedom resulting from a joint optimization of the RF pulse segments.

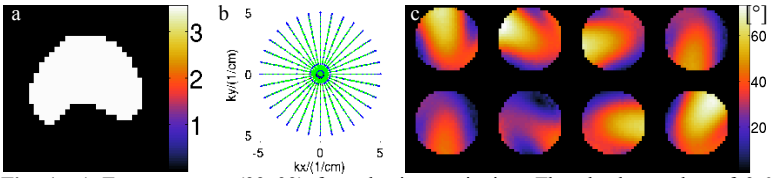

Fig. 1: a) Target pattern (32x32) for selective excitation. The absolute value of 3.6 reflects the transverse magnetization adding constructively during 16 excitations. b) trajectory in TX k-space with 16 segments (accelerated by a factor of 3 compared to full radial sampling) c) Flip angle maps, acquired in a water bottle phantom on a 3T Siemens Magnetom Trio with 8-channel TxArray extension, used for parallel transmit acceleration

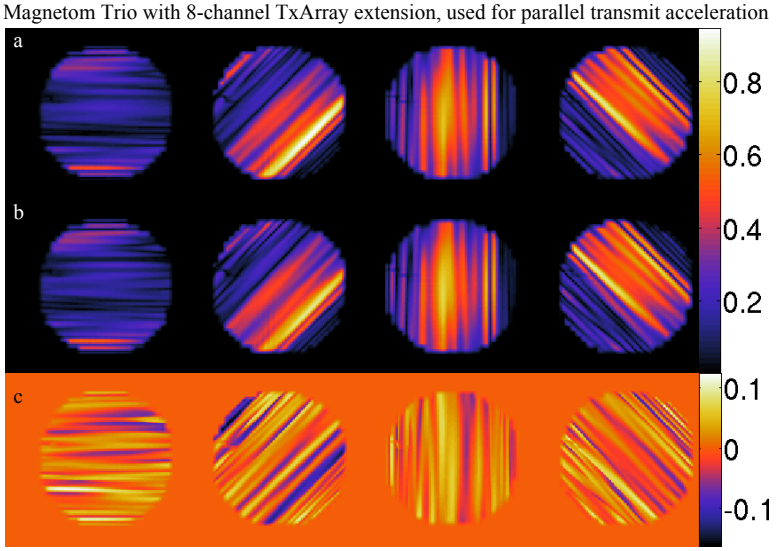

Fig. 2: Magnetization patterns $M_s(T, \mathbf{r})$ for four individual segments out of 16. a) Patterns resulting from the previous segment-wise optimal control design b) Patterns resulting from the generalized nonlinear pulse design. c) Difference maps b-a.

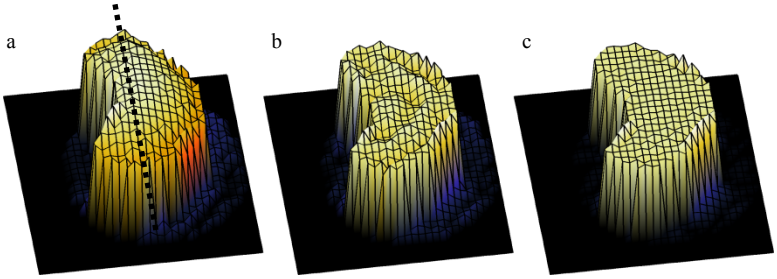

Fig. 3: Simulations of transverse magnetization generated by the complete set of 16 RF pulse segments. a) Small tip angle design b) Segment-wise optimal control design c) Generalized optimal control design. The dotted line indicates a section along which the magnetization profile is given quantitatively in Fig. 4.

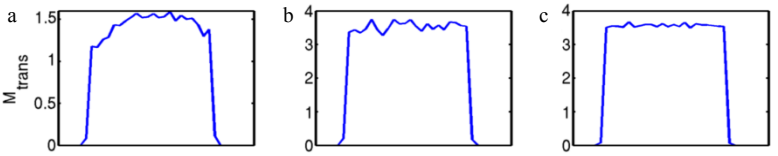

Fig. 4: Sections through the simulation in Fig. 3 along the direction marked by the dotted line. a) Small tip angle design b) Previous segment-wise optimal control design c) Generalized optimal control design

References

[1] W. Grissom et al., MRM **56**, 620 (2006). [2] M. Haas et al., Proc. ISMRM, p2589 (2009). [3] U. Katscher et al., Magn Reson Med **49**, 144 (2003). [4] Y. Zhu, Magn Reson Med **51**, 775 (2004). [5] P. Ullmann et al., MRM **54**, 994 (2005). [6] Q. Qin et al., Magn Reson Med **58,** 19 (2007). [7] J. Snyder et al., Magn. Reson, Med early view, DOI: 10.1002/mrm; [8] D. Xu, MRM **59**, 547 (2008).

Acknowledgment This work is a part of the INUMAC project supported by the German Federal Ministry of Education and Research, grant #13N9208.